Acid Hydrotropic Fractionation of Lignocelluloses for Sustainable Biorefinery: Advantages, Opportunities, and Research Needs

Junyong Zhu,*[a] Liheng Chen,[b] and Cheng Cai[c]

This Minireview provides a comprehensive discussion on the potential of using acid hydrotropes for sustainably fractionating lignocelluloses for biorefinery applications. Acid hydrotropes are a class of acids that have hydrotrope properties toward lignin, which helps to solubilize lignin in aqueous systems. With the capability of cleaving ether and ester bonds and even lignin-carbohydrate complex (LCC) linkages, these acid hydrotropes can therefore isolate lignin embedded in the plant biomass cell wall and subsequently solubilize the isolated lignin in aqueous systems. Performances of two acid hydrotropes, that is, an aromatic sulfonic acid [*p*-toluenesulfonic acid (*p*-TsOH)] and a dicarboxylic acid [maleic acid (MA)], in terms of delignification and dissolution of hemicelluloses, and reducing lignin condensation, were evaluated and compared. The advantages of lignin esterification by MA for producing cellulosic sugars through enzymatic hydrolysis and lignin-containing cellulose nanofibrils (LCNFs) through mechanical fibrillation from the fractionated water insoluble solids (WIS), and for obtaining less condensed lignin with light color, were demonstrated. The excellent enzymatic digestibility of maleic acid hydrotropic fractionation WISs was also demonstrated by comparing with WISs from other fractionation processes. The recyclability and reusability of acid hydrotropes were also reviewed. Finally, perspectives on future research needs to address key technical issues for commercialization were also provided.

1. Introduction

Lignocellulosic plant biomass is a renewable bioresource that can be sustainably produced in large quantities in many regions of the world. In the United States alone, a billion tons of plant biomass can be produced annually.[1] Currently, commercial utilization of plant biomass is primarily limited to producing paper and dissolving fibers from wood in the pulp and paper industry. Herbaceous or agricultural plant biomass has been largely underutilized; it has mainly been used for fuels through burning or used as animal bedding or soil conditioners.[2,3] Plant biomass has a diverse chemical composition and consists of long chain polysaccharides that have high mechanical strength as well as aromatic ring-structured lignin. These molecules can be used to produce a variety of bioproducts, biofuels, and biochemicals through the biorefinery concept to replace petroleum-based products, fuels, and chemicals.[4,5] Because plant biomass can sequester carbon, the successful development of plant biomass biorefinery can decrease carbon footprint and achieve sustainable economic development. Sustainable fractionation of plant biomass into usable building blocks for conversion to platform molecules[4,6] is the key to attain this goal. Because the upstream fractionation process also dictates the technologies for downstream processing and waste stream treatment, developing viable and sustainable fractionation technologies is critically important.

Much research and development efforts have been made in plant biomass fractionation. Most noticeable are the commercial wood pulping process for producing cellulosic fibers using alkaline or sulfite delignification and the variants of this process,[7–9] along with the classical dilute acid fractionation[10,11] and steam explosion[12–14] for producing sugars from the carbohydrate fraction. Other methods include ammonia[15,16] and organic solvents.[17–19] High reaction temperatures of approximately 130–170 °C for a period of 1–4 h are applied to achieve maximal delignification in commercial wood pulping. Similarly, high temperatures are also applied in the previously mentioned fractionation processes to maximize enzymatic sugar yield. Consequently, the resultant dissolved and retained lignin in the lignocellulosic solid fraction are highly condensed with low reactivity, similar to commercial technical lignin from wood pulping.[20,21] Lignin condensation is a significant barrier to the use of lignin as a key building block for producing platform molecules for biorefinery.[22,23]

Recent progress in developing fractionation processes included finding novel and better solvent systems, such as organic co-solvent systems using γ-valerolactone (GVL)[24] and tetrahydrofuran (THF),[25] ionic liquid (IL),[26–29] and deep eutectic solvent (DES) systems.[30,31] Although these systems are effective in efficiently solubilizing lignin and/or hemicelluloses to obtain

[a] Dr. J. Zhu
USDA Forest Service
Forest Products Laboratory
Madison, WI (USA)
E-mail: junyong.zhu@usda.gov
[b] Dr. L. Chen
Department of Biomedical Engineering
Jinan University
Guangzhou (P. R. China)
[c] Dr. C. Cai
Dalian Institute of Chemical Physics
Chinese Academy of Sciences
Dalian (P. R. China)

© 2021 The Authors ChemSusChem
© 2021 Chemistry Europe and Wiley-VCH GmbH.
This article has been contributed to by US Government employees and their work is in the public domain in the USA.

highly digestible cellulosic fraction for enzymatic sugar production, the resultant lignin from most of these solvent systems was condensed except when fractionation was conducted under mild conditions, which decreased the enzymatic digestibility of the fractionated solids.[21,32–35] Moreover, the significantly higher costs of GVL, IL, and THF compared with conventional alkali and mineral acids, along with the higher dosages (concentrations) needed for these solvents to be effective, require a very high chemical recovery efficiency that is too difficult to achieve for economical biorefinery operations. Furthermore, despite the fact that some of these solvents have been called "green" (such as ILs for their negligible vapor pressure, which eliminates inhaling risk), even a minor inefficiency in chemical recycling can be an environmental concern because of the great dosages applied for achieving required efficacy in biorefinery operation at the scale of a thousand tons of plant-biomass per day. Most ILs can pose serious threats to aquatic and terrestrial ecosystems because they mostly have a certain level of solubility in water.[36] DESs are regarded as "green" for their eco-friendly H-bond donors; however, cholinium-based DESs that are often used for fractionating lignocelluloses have strong antibacterial activities and significant toxic effects on living organisms.[37] Despite low toxicities of these solvents such as THF, considering that toxicity profiles and detailed human toxicity and risk assessments of these chemicals are lacking,[37–39] the effects of large-quantity usage of these solvents in biorefinery operations on environmental sustainability remains uncertain.

Reductive catalytic lignin fractionation (RCF)[23,40] was recently applied to lignocelluloses to avoid lignin condensation by directly catalyzing plant biomass to depolymerize native lignin into monomers or aromatics in one step. However, RCF often requires organic solvents and high temperatures of 170 °C[41] and therefore has similar issues associated with chemical recovery and environmental impact to using organic solvents. Furthermore, valorization of carbohydrates of approximately 65% of the lignocellulosic biomass remains unaddressed[23,42–44] with only limited efforts being made.[45–47] Issues associated with recycling of catalysts that remain mixed with the carbohydrate fraction also need to be fully resolved.[23,40,48]

In view of this discussion, the conventional two-step approach, that is, fractionation first, such as wood pulping, followed by lignin valorization, can be an attractive pathway as long as fractionation can avoid substantial lignin condensation.[49] Acid hydrotropic fractionation (AHF), recently developed by Zhu and co-workers at the USDA Forest Service, Forest Products Laboratory,[50,51] was aimed at addressing critical issues associated with existing fractionation processes, including lignin valorization by reducing lignin condensation, chemical recovery, and environmental impact by using aqueous systems and chemicals with low solubility and minimal or no toxicity, as well as great fractionation selectivity for efficient conversion of resultant building blocks to platform molecules or directly to biomaterials or biochemicals. AHF also has other advantages. For example, the dissolved lignin can be separated simply through dilution using water, fractionation is operated at atmospheric pressure and low temperatures to reduce capital cost, and the dissolved hemicelluloses can be directly dehydrated into furan using the hydrotrope in the fractionation liquor without additional catalysts. Furthermore, one acid hydrotrope, maleic acid (MA), is a U.S. Food and Drug Administration (FDA) approved indirect food additive (21CFR175-177). Therefore, trace amounts of MA remaining in

Dr. J.Y. Zhu received his Ph.D. from the University of California-Irvine. He was a faculty member at the Institute of Paper Science and Technology, Atlanta, Georgia, from 1993 to 2003. Currently he is a scientific leader at the USDA Forest Products Laboratory with an adjunct appointment at the University of Wisconsin-Madison. His research includes broad area of wood and fiber utilization from laboratory studies to commercial scale demonstrations. Dr. Zhu was the Fulbright-Aalto University Distinguished Chair in 2016. Recognitions of his accomplishments include the IUFRO Scientific Achievement Award, USDA Undersecretary and USFS Chief honor awards, AIChE Andrew Chase award, TAPPI Aiken Prize.

Dr. Liheng Chen received his B.Sc. from the South China University of Technology in 2010 and his Ph.D. from the same university in 2016. He was a visiting Ph.D. student and post-doctoral fellow at the USDA Forest Products Laboratory, Madison, Wisconsin USA, from 2013 to 2016 under Dr. J.Y. Zhu. He joined Jinan University, Guangzhou, China in 2016 as Research Associate. His research interests include fractionation of lignocellulose and applications of fractionation key building blocks.

Dr. Cheng Cai received his B.Sc. from Wuhan Institute of Technology in 2014, and his Ph.D. from South China University of Technology in 2020. He was visiting Ph.D. student in Dr. J.Y. Zhu's group at the USDA Forest Products Laboratory, Madison, Wisconsin, USA from 2018 to 2020. Currently, he is a post-doctoral fellow in Dr. Feng Wang's group at the Dalian Institute of Chemical Physics, Chinese Academy of Sciences, Dalian, China. His research interests mainly include fractionation and enzymatic hydrolysis of lignocellulose, production and application of cellulose nanomaterials.

© 2021 The Authors ChemSusChem
© 2021 Chemistry Europe and Wiley-VCH GmbH.
This article has been contributed to by US Government employees and their work is in the public domain in the USA.

the fractionated products or process streams are deemed safe to human health and ecosystems, which helps achieve true environmental sustainability. In view of these advantages, the goal of this Minireview is to provide a summary of existing literature on AHF to attract broad interest for potential commercial biorefinery applications and point out future research needs.

2. Mechanism of Acid Hydrotropic Fractionation of Lignocelluloses

2.1. Intrinsic properties of hydrotropes

Hydrotropic phenomenon was discovered in 1916 by Neuberg.[52] It refers to solubilization of hydrophobic materials in aqueous systems by hydrotrope aggregation around the solute.[53–55] Current applications are mainly in the pharmaceutical industry.[56] Hydrotropes function similar to surfactants and chaotropic agents.[57,58] Even today, the differentiation from chaotrope to hydrotrope[57] and from hydrotrope to surfactant[59] is not clear-cut. For example, urea is reported as a chaotrope[60] but is sometimes listed as a hydrotrope to describe the solubility-enhancing effect.[56,57] Also, sodium *p*-toluenesulfonate (STS) and sodium dodecyl benzene sulfonate (SDBS) are classical hydrotrope and surfactant, respectively, with a clear distinction in their length of amphiphilic alkyl moieties.[59] Even though the boundary between hydrotrope and surfactant is ambiguous, their intrinsic behaviors are well described. Usually, surfactant molecules have a long amphiphilic tail and aggregate to form a microemulsion in water when their concentration exceeds the critical micelle concentration (CMC), whether a hydrophobic solute is present or not.[57] In contrast, chaotropic agents are strongly hydrophilic and may not aggregate.[61] Interestingly, the hydrotropic molecules slightly aggregate when their concentration is above the minimum hydrotrope concentration (MHC), and the aggregation is enhanced in the presence of hydrophobic compounds.[56]

In general, the solubilization of hydrophobic solute in water increases with the increase in hydrotrope concentration. However, surfactants form abundant well-defined micellar structures at high concentration, at which the heterogeneous solvent system may impair the solubilization and subsequent reactivity of solute.[62] In comparison with chaotrope, hydrotropes exhibit an MHC above which hydrophobic solutes can be dissolved in aqueous hydrotropic solution and below which solutes can be precipitated. This behavior of hydrotropes around MHC suggests that using hydrotropes can realize the dissolution, separation, and purification of hydrophobic solute in one pot. Of special note, MHC can be easily determined via measuring the conductivity of hydrotrope solutions in a range of concentrations.[59,63] However, it should be pointed out that the solubility curve versus hydrotrope concentration is sigmodial without a sharp transition point based on analysis using statistical thermodynamics.[64] Therefore, 100% separation and recovery of solute through precipitation is not possible.[65]

Acid hydrotropes are molecules that simultaneously possess the properties of acid and hydrotrope. They not only can catalyze hydrolysis reactions but also dissolve and purify the hydrophobic compounds in water. When applied to lignocelluloses, an acid hydrotrope acts as an acid to cleave ether/ester linkages to depolymerize and dissolve hemicelluloses into sugars. However, it only produces a minor depolymerization of cellulose that remains as an insoluble solid under most fractionation conditions due to the strong β-1-4 linkage and highly hydrogen-bonded cellulose structure. The term acid hydrotrope fractionation was first proposed and applied to fractionate lignocelluloses only recently by Zhu and co-workers at the USDA Forest Service, Forest Products Laboratory.[50] They used *p*-toluenesulfonic acid (*p*-TsOH) to fractionate a variety of plant biomass, such as wood[66,67] as well as herbaceous and forest biomass.[68,69] They also found some novel acid hydrotropic agents such as MA[51] that can also functionalize lignin for efficient fractionation.

2.2. Mechanism of acid hydrotropic fractionation of lignocelluloses

To understand and confirm the hydrotrope aggregation mechanism in solubilizing solute in hydrotropic systems, Abranches et al. conducted an experimental and computational study using gallic acid and syringic acid as solutes but with very different hydrophobicities, and monoalkylglycerol ethers as hydrotrope that can be made to varied length in their alkyl chain.[55] They explained that the aggregation of hydrotrope molecules around a solute is driven by the strong water-mediated (or hydrotropic) interaction between the hydrotrope and solute because the interaction of the apolar (or hydrophobic) moiety of a hydrotrope molecule with water is much weaker than a water-water hydrogen bond.[55] Furthermore, they explained that there can be three scenarios in hydrotrope-solute systems: (1) apolarity of the hydrotrope is small and the driving force for aggregation is low; (2) apolarity of the hydrotrope is equal to that of the solute and the driving force for aggregation around the solute is maximized; (3) apolarity of the hydrotrope is greater than that of the solute to result in more hydrotropes-hydrotrope aggregation than hydrotropes-solute aggregation. They therefore concluded that the driving force for hydrotrope aggregation around a solute is the balance between the apolarity of both solute and hydrotrope.

Based on this mechanism, acid hydrotrope can aggregate around isolated/separated lignin molecules via van der Waals (vdW) interaction to prevent lignin from aggregation. Studies illustrated the π-π (strong vdW forces) and CH-π interactions between hydrotropes and lignin molecules using both experimental and computational methods.[70–73] Apparently, the acid hydrotropes that have been evaluated, such as *p*-TsOH and MA,[50,51] are rich in π electrons.

In lignocelluloses, lignin is embedded in the carbohydrate matrix rather than isolated. For decades, studies have proposed that significant lignin moieties covalently bonded with carbohydrates are created through the formation of lignin carbohydrate

© 2021 The Authors ChemSusChem
© 2021 Chemistry Europe and Wiley-VCH GmbH.
This article has been contributed to by US Government employees and their work is in the public domain in the USA.

complexes (LCCs) as shown in Figure 1A.[74–76] However, recent studies on secondary plant cell walls indicated that lignin and xylans tend to form their own separate phases with limited interpenetration and chemical bonding or formation of LCCs as shown in Figure 1B.[77–79] Even though the interacting forms between lignin and hemicelluloses are still under debate,[75] it is understood that freeing the embedded lignin from the carbohydrate matrix by destroying the covalent or noncovalent bonds between them is a necessary step for delignification. Certainly, depolymerizing and removing hemicelluloses can also expose the embedded lignin to facilitate the extraction of lignin by solvents. Acid hydrotrope as an acid can be strong enough to cleave the linkages in LCCs including benzylether, benzyl ester, ferulate ester, and others, (Figure 1A) and hydrolyze lignin-bound hemicelluloses (Figure 1B) to liberate the bonded and trapped lignin. The cleaved lignin along with the naturally separated lignin phase embedded in plant biomass can then be dissolved in water by the aggregation of acid hydrotrope molecules that have hydrophilic ends. As illustrated in Figure 1C,[50] *p*-TsOH was applied to catalyze hydrolysis of ether and/or ester bonds in hemicelluloses and LCCs to isolate lignin. The phenomenon of acid hydrotrope aggregation around lignin

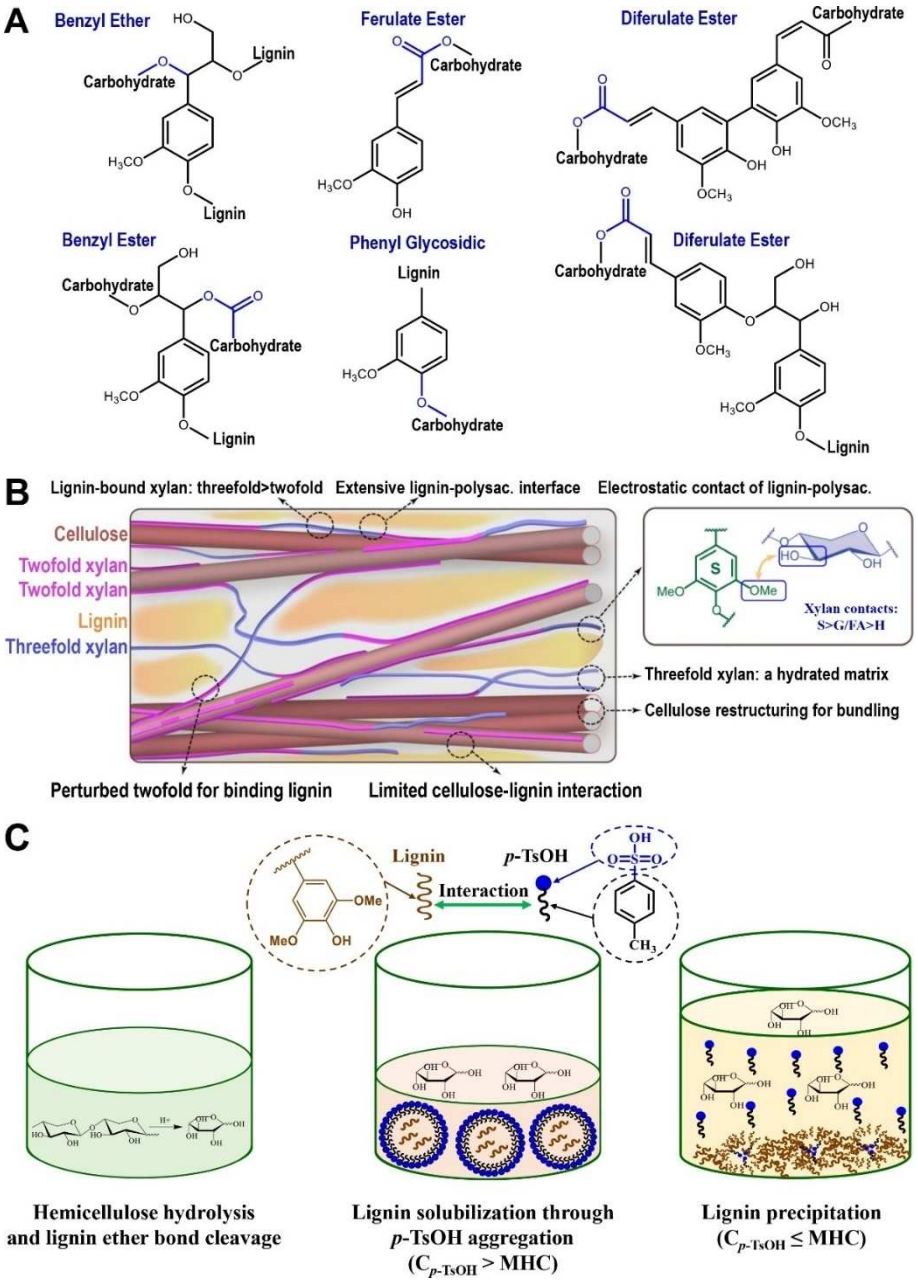

Figure 1. (A) Different chemical linkages between lignin and carbohydrates in lignocelluloses structures. Reprinted with permission from ref. [74]. Copyright 2018, Springer. (B) Secondary cell wall model. Reprinted with permission from ref. [78]. Copyright 2019, Springer. (C) Carbohydrate and lignin solubilization by *p*-TsOH ($C_{p\text{-TsOH}} > MHC$) and precipitation ($C_{p\text{-TsOH}} \leq MHC$). Reprinted with permission from ref. [50]. Copyright 2017, American Association for the Advancement of Science.

© 2021 The Authors ChemSusChem
© 2021 Chemistry Europe and Wiley-VCH GmbH.
This article has been contributed to by US Government employees and their work is in the public domain in the USA.

as discussed may improve the acid-catalyzed hydrolysis reaction in theory. Therefore, the synergistic effect of the hydrotropy phenomenon on acid hydrolysis of ether and/or ester bonds cleavage can promote the separation and isolation of lignin from the plant cell wall matrix for effective dissolution. Dilution with water destroyed aggregation, which resulted in lignin precipitation.

3. Performance of Acid Hydrotropic Fractionation of Lignocelluloses

Using aromatic sulfonic salts such as sodium xylenesulfonate as hydrotrope to dissolve lignin for wood pulping was practiced in the 1940 s[80] but never commercialized due to low fiber yields, inferior fiber mechanical properties, and very long cooking times of 11–12 h at high temperatures of 150 °C.[81] Recent studies on hydrotropy included using aromatic sulfonic salts to fractionate lignocelluloses for enzymatic sugar production. However, the enzymatic digestibility of the resultant water-insoluble solids (WIS) was only approximately 50% with a moderate cellulase loading of 10 FPU (g substrate) ^{1} [≈20 FPU (g glucan) ^{1}] after birch wood was fractionated using sodium xylenesulfonate at 150 °C for 120 min.[82] The high fractionation temperature also substantially condensed dissolved lignin with low content of ether aryl β-O-4′ linkages.[83] It can be concluded that aromatic sulfonic salt based hydrotropic fractionation of lignocelluloses was not effective.

AHF refers to fractionating lignocelluloses using a group of acids with hydrotropic properties, as opposed to using salts that have been exclusively studied.[81,84] AHF was carried out following the schematic flow diagram shown in Figure 2. Elevated acid concentrations above MHC raised the boiling point of the fractionation liquor to allow fractionation to be carried out at atmospheric pressure even at temperatures >100 °C. Acid hydrotropes have excellent selectivity in preserving cellulose and dissolving lignin. As acids, they also substantially solubilize hemicelluloses to result in a WIS with high cellulose content and low lignin and hemicellulose content.[50,51]

The separation and recovery of the dissolved lignin can be achieved simply by diluting the fractionation liquor to below MHC using water. Furthermore, the dissolved lignin has a low extent of condensation because of the low fractionation temperatures and short fractionation time. The dissolved hemicellulosic sugars can be dehydrated into furan with high yield using the hydrotrope in the fractionation liquor without additional catalysts.[67,85] The sugar-dehydrated liquor that contains mainly the hydrotrope can then be reused. Therefore, AHF can efficiently fractionate all three major components of lignocelluloses with only one chemical at atmospheric pressure and is advantageous for plant biomass biorefinery applications.

3.1. AHF for biorefining lignocelluloses using aromatic sulfonic acid

Several aromatic sulfonic salts have hydrotropic properties,[84] as do several aromatic sulfonic acids. *p*-TsOH was first used to fractionate poplar wood by Chen et al.[50] In that study, poplar wood chips were first Wiley-milled to 20 mesh and then fractionated at acid concentration 70–85 wt% and temperature 50–80 °C for 5–60 min at a liquor/wood ratio of 10:1 (mL g ^{1}). At the end of each fractionation run, the fractionated WIS were separated from spent liquor through filtration. The WIS were washed using water. Mass balance of selected fractionation runs from the study are listed in Table 1. More than 90% delignification and more than 85% xylan dissolution were achieved in the run P80T80t20, which stands for reaction at *p*-TsOH concentration 80 wt% and 80 °C for 20 min. Even in run P75T65t05 with 5 min fractionation at 65 °C, more than 57% delignification and 70% xylan dissolution were achieved. More than 80% of cellulose were retained in both conditions. These numbers indicate that AHF using *p*-TsOH is highly selective and rapid. It is also noted that most of the dissolved xylan were in the form of monomeric xylose especially at high fraction severities with low furfural production. Only a small amount of removed cellulose was converted into glucose, and most removed cellulose was in the form of oligomeric glucose.

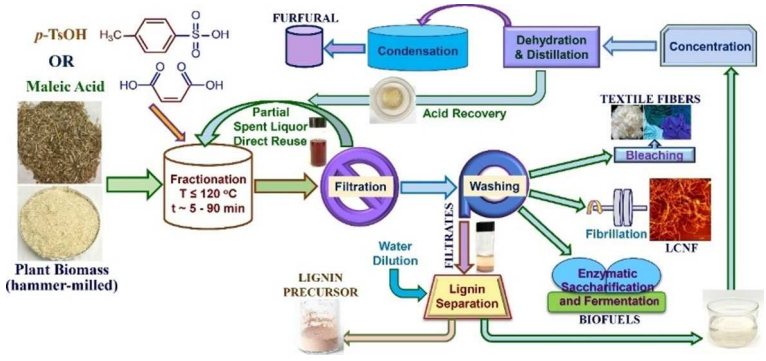

Figure 2. Schematic flow diagram showing AHF of lignocelluloses for producing cellulosic fibers, nanomaterials, sugars, lignin with low degree of condensation, and furfural with acid recovery and reuse. Adapted from with permission from ref. [50]. Copyright 2017, American Association for the Advancement of Science.

© 2021 The Authors ChemSusChem
© 2021 Chemistry Europe and Wiley-VCH GmbH.
This article has been contributed to by US Government employees and their work is in the public domain in the USA.

Sample label[a]	WIS					Spent liquor				
	Solids yield [%]	Glucan [%]	Xylan [%]	Mannan [%]	Lignin [%]	Glucose [g L^{-1}]	Xylose [g L^{-1}]	Mannose [g L^{-1}]	Acetic acid [g L^{-1}]	Furfural[b] [g L^{-1}]
untreated poplar	100	45.7	14.9	4.6	23.4	–	–	–	–	–
P70T50t35	74.4	62.2 (101.1)	7.4 (37.0)	4.3 (68.9)	19.2 (61.0)	1.1 (2.2)	8.9 (52.4)	1.0 (20.3)	1.1	0.05 (0.5)
P70T65t35	64.1	68.0 (95.3)	6.6 (28.4)	4.6 (64.0)	13.0 (35.7)	1.3 (2.5)	10.1 (59.5)	1.5 (29.9)	1.5	0.08 (0.7)
P70T80t35	55.5	67.3 (81.7)	4.9 (18.3)	4.2 (50.5)	6.7 (15.8)	1.8 (3.6)	11.6 (68.3)	2.0 (38.7)	1.5	0.19 (1.7)
P70T80t20	58.9	63.0 (81.1)	6.5 (24.5)	4.3 (53.8)	8.8 (22.1)	1.5 (3.0)	11.0 (65.0)	1.8 (35.2)	1.6	0.13 (1.2)
P75T65t05	67.1	56.2 (82.4)	6.5 (29.3)	4.1 (60.0)	15.0 (42.9)	1.2 (2.4)	10.1 (59.7)	1.5 (29.3)	1.5	0.07 (0.6)
P75T65t20	60.7	71.8 (95.4)	5.8 (23.8)	4.9 (63.7)	10.8 (28.0)	1.4 (2.7)	10.8 (64.0)	1.7 (32.4)	1.5	0.10 (0.9)
P75T65t35	59.0	71.7 (94.5)	6.0 (23.9)	4.0 (51.3)	8.9 (22.3)	1.3 (2.6)	10.3 (60.8)	1.7 (32.4)	1.4	0.10 (0.9)
P75T65t60	57.0	74.7 (93.1)	5.0 (19.2)	4.3 (52.8)	7.4 (17.9)	1.7 (3.2)	10.7 (63.4)	1.8 (34.6)	1.5	0.14 (1.2)
P75T80t20	55.0	72.4 (87.1)	5.2 (19.1)	4.4 (52.7)	6.1 (14.4)	1.8 (3.6)	10.9 (64.2)	2.0 (39.7)	1.5	0.19 (1.7)
P80T80t20	51.9	72.3 (81.9)	3.7 (13.0)	3.7 (41.8)	4.2 (9.2)	2.3 (4.6)	9.9 (58.4)	2.2 (43.9)	1.4	0.33 (3.1)

[a] P*xx*T*yy*t*zz* stands for fractionation conditions: *p*-TsOH concentration in *xx* wt% at *yy* °C for *zz* min. [b] Yields are based on xylan content in poplar wood. HMF in spent liquors was not detectable. The numbers in the parentheses are component yields based on components in the untreated poplar.

After centrifugation, precipitation of dissolved lignin by diluting the fractionated liquor to below MHC can be clearly seen from the photo in Figure 3A with dilution to 10 wt% slightly below the *p*-TsOH MHC of 11.5 %.[50] It can also be seen from the changes in the dynamic light scattering (DLS) measured effective lignin particle size with dilution. DLS lignin particle size showed a slow graduate increase with dilution and then a sharp increase when the liquor was diluted to 10 wt%. Atomic force microscopy (AFM) imaging revealed that the lignin in the diluted fractionation liquor of 10 wt% was in the form of aggregated lignin nanoparticles (LNPs) due to the loss of hydrotropic effect at *p*-TsOH concentration below MHC (Figure 3B). Removing the aggregates through centrifugation retained only primary particles in the supernatant of the diluted liquor (Figure 3C). Increasing centrifugation force removed more aggregates (Figure 3D). The colloidal primary particles have a thickness of approximately 3 nm based on AFM topographical measurements with a lateral dimension of 50 nm (Figure 3C,D). Ma et al. found that many factors affect the physical dimensions of the LNPs from AHF including dilution speed, ionic strength, and others,[86] and therefore can be used to control LNP size. Colloidal LNPs have many applications.[87] However, existing LNPs were produced from commercial technical lignin that contained sulfur and metals using solvent systems. Hydrotropic fractionation can produce colloidal LNPs directly from lignocelluloses with good purity.

With the removal of lignin and dissolution of hemicelluloses, the fractionated cellulosic WIS were readily digestible by enzymes to produce glucose. Substrate enzymatic digestibility (SED) of poplar wood WIS from P75T80t20 reached approximately 90 % at cellulase loading of 15 FPU (g glucan)$^{-1}$ (Figure 3E).[50] Coproduction of bioethanol from poplar wood WIS fractionated using *p*-TsOH and furfural from the dissolved xylose through direct dehydration of the AHF spent liquor without any additional catalyst was also demonstrated recently.[67] Simple batch distillation produced a good furfural yield of 78 %.

AHF-fractionated WIS using *p*-TsOH was also evaluated for producing lignin-containing cellulose nanofibrils (LCNFs) directly from birch wood.[88] Under the fractionation condition of P50T80t20, the WIS were readily fibrillated to LCNFs even with one pass (low energy input) through a microfluidizer as shown in Figure 3F. Increasing fibrillation decreased the thickness of the fibrils from approximately 70 nm (one pass) to approximately 23 nm after seven passes through microfluidization (Figure 3G,H). The extent of fibrillation applied was much lower than the 30 passes required to fibrillate a bleached kraft eucalyptus pulp to similar thickness.[89]

The initial batch study found that dissolved lignin from AHF had a low degree of condensation. For batch AHF, approximately two-thirds of β-O-4′ ether aryl linkages in poplar wood lignin can be preserved at 50 % delignification.[90] The rapid AHF allowed efficient fractionation using flow-through reactors to further decrease lignin condensation.[49] As illustrated in Figure 4A, AHF-dissolved lignin (AHL) contains higher β-O-4′ ether aryl linkages compared with technical lignin[22,91] under the same extent of delignification. Furthermore, AHL from a flow-through reaction has even less condensation than AHL from a batch reaction.[90]

The lower extent of AHL condensation can also be seen from the color of the AHL. The AHL from flow-through reaction tends to have pinkish color compared with the dark brown color from Kraft pulping (Figure 4B1–B5). Reaction product 1-hydroxy-3-(4-hydroxy-3-methoxyphenyl)-2-propanone (HHMP)

© 2021 The Authors ChemSusChem
© 2021 Chemistry Europe and Wiley-VCH GmbH.
This article has been contributed to by US Government employees and their work is in the public domain in the USA.

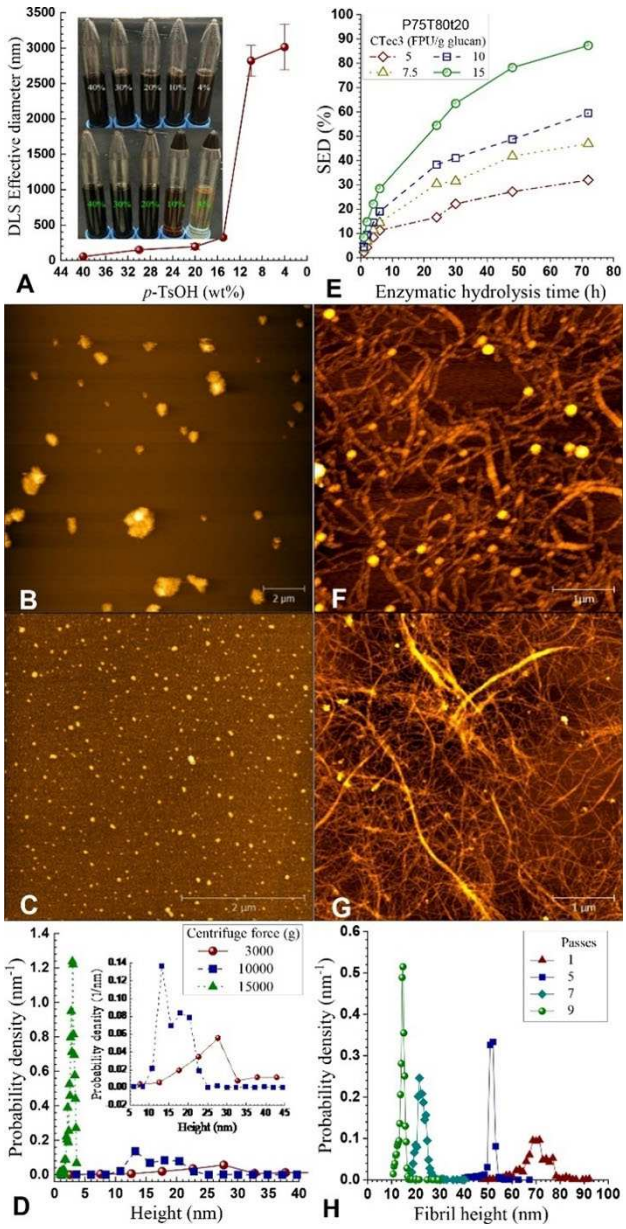

Figure 3. (A–D) Lignin nanoparticles and (E) sugar production from poplar wood by AHF under P75T80t20. Reprinted with permission from ref. [50]. Copyright 2017, American Association for the Advancement of Science. (F–H) Lignin containing cellulose nanofibrils from birch under P50T80t20. Reprinted with permission from ref. [88]. Copyright 2017, Royal Society of Chemistry. Scale bars: 2 μm (B,C) and 1 μm (F,G).

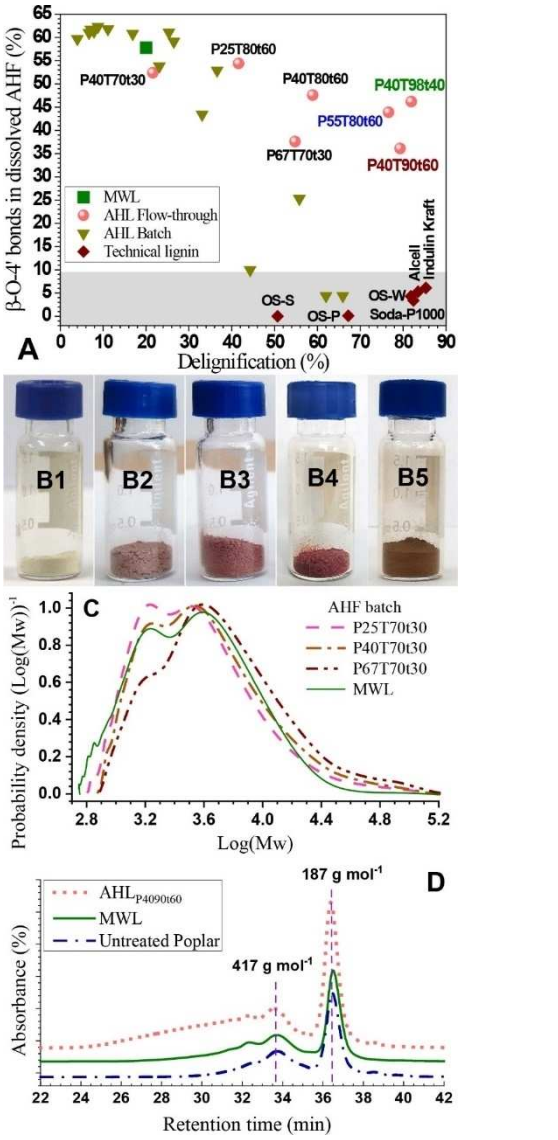

Figure 4. Characterization and catalytic conversion of poplar AHLs dissolved by *p*-TsOH. (A) Extent of condensation measured by β-O-4′ ether aryl linkages from 2D ^{1}H ^{13}C NMR analysis. (B1–B5) Images of poplar AHL samples from flow-through AHF at different severities in comparison with poplar MWL and a commercial Kraft lignin. (B1) MWL (yield = 20%); (B2) P25T80t60 (41.6%); (B3) P55T80t40 (74.8%); (B4) P40T98t40 (81.8%); (B5) Kraft (84.8%). (C) Comparison of molecular weight distribution of poplar AHL from different batch fractionation runs. (D) Comparison of a poplar flow-through AHL from P40T90t60 with MWL and untreated poplar for aromatics production through catalysis. Reprinted with permission from ref. [49]. Copyright 2019, American Chemical Society.

was identified from cleavage of β-O-4′ ether bonds in acidolysis of model lignin guaiacylglycerol-β-guaiacyl ether (GG) in 40 wt % *p*-TsOH at 90 °C. HHMP is one of the Hibbert's ketones (HK) from depolymerization[92,93] and identified in 2D NMR spectra of AHL at δ_C/δ_H 67.1/4.19 ppm.[49,90] The conjugated double bond and aldehyde auxochrome group in the coniferyl aldehyde[94] formed through the dehydration of HHMP along with the ketone auxochrome group in HHMP contribute to the pinkish color.[95]

Increasing lignin condensation with delignification or AHF severity also can be seen from AHL molecular weight (M_w) distribution measured by gel-permeation chromatography (GPC). As shown in Figure 4C, M_w distribution shifted to higher molecular weight as AHF severity increased. Furthermore, the second peak at a higher M_w became more pronounced. Both were results of AHL repolymerization or condensation. With the use of Ru/C depolymerization, AHL from flow-through AHF P40T90t60 was found to produce good yield of lignin aromatics,

© 2021 The Authors ChemSusChem
© 2021 Chemistry Europe and Wiley-VCH GmbH.
This article has been contributed to by US Government employees and their work is in the public domain in the USA.

similar to the results from milled wood lignin (MWL) or untreated poplar with a major monomer peak at 187 g mol $^{-1}$ and a dimer peak at 417 g mol $^{-1}$ in the GC-MS as shown Figure 4D. The AHL sample produced a slightly broader distribution than the MWL or untreated poplar did due to lignin condensation with β-O-4′ = 36.1% compared with 57.8% for MWL.

3.2. Lignin esterification in maleic acid hydrotropic fractionation

Recently, Cai et al. found that MA, a dicarboxylic acid, has strong hydrotropic properties toward poplar wood lignin.[51] As previously mentioned, MA is a U.S. FDA-approved indirect food additive. It also has lower solubility in water and is a much weaker acid than aromatic sulfonic acids such as *p*-TsOH, which can substantially facilitate acid recovery and achieve true environmental sustainability. In addition to these advantages, maleic acid hydrotropic fractionation (MAHF) has a unique feature of esterification reactions with lignocelluloses, in addition to all the features of AHF using aromatic sulfonic acids. It is well known that carboxylic acids can esterify cellulose through the Fischer-Speier reaction.[96] Fourier-transform infrared (FTIR) spectroscopy and conductometric titration indicated esterification or carboxylation of cellulose nanocrystals produced by MA hydrolysis of bleached kraft pulp fibers at 50–75 wt% and 100–120 °C for more than 30 min.[97,98] These reaction conditions are similar to typical MAHF experiments.

Furthermore, 2D ^{1}H ^{13}C heteronuclear single quantum coherence (HSQC) NMR analysis indicated that MAHF can esterify dissolved poplar wood lignin (MAHL).[51] Under mild fractionation, MAHL samples have similar spectra to that of MWL with well-preserved β-O-4′ ether aryl linkages except those containing carbohydrates, suggesting incomplete cleavage of LCCs. Increasing fractionation severity decreased carbohydrate content, β-O-4′ linkages, and MAHL molecular weight.[51] Furthermore, new strong signals in the aromatic region at δ_C/δ_H 127.8/6.2 and 133.2/6.4 ppm and in the aliphatic region at 64.2/4.2 ppm were observed. Literature NMR studies demonstrated that model lignin GG can be esterified by formic acid or acetic acid at the γ-position with aliphatic HSQC signals for γ (^{13}C ^{1}H) at 63.5/(3.83, 4.30) and 62.1/(4.23, 4.43) ppm,[99–101] respectively. Cai et al. therefore used model lignin GG to react with MA under M60T100t60 (MA concentratioon 60 wt% at 100 °C for 60 min).[51] They observed GG-MA reaction product at δ_C/δ_H 63.6/(4.03, 4.39) ppm, as shown in Figure 5A. Furthermore, the MA signal at 130.8/6.3 ppm disappeared and two strong peaks appeared at δ_C/δ_H 128.0/6.2 and 132.9/6.4 ppm after reaction with GG. This is consistent with esterification and presumably at the γ-position because the primary ester is more stable.[102] Cai et al. then conducted a long-range heteronuclear multiple bond correlation (HMBC) NMR experiment on the GG-MA reaction product to verify esterification at the γ-position.[51] They clearly observed the γ protons have a three-bond correlation to the C1 carbonyl of MA as circled in Figure 5B. They also verified lignin carboxylation using ^{31}P NMR measurements of MAHL samples. As listed in Table 2, the carboxyl group content in dissolved MAHL increased with increasing fractionation severity due to esterification.[103] Carboxyl group content of 0.61 mmol g $^{-1}$ was obtained under M70T80t30 with the highest MA concentration because esterification reaction always proceeds further with less water. The carboxyl group content in all dissolved lignin samples is higher than that reported for cellulose when lignin-free cellulosic fibers were reacted with dicarboxylic acids under similar or more severe reaction conditions.[97,98] Carboxylated lignin with a low degree of condensation is advantageous for high-value valorization due to its ability to be modified for various applications.[104,105]

MA also oxidizes the OH group in MAHL. Compared with MWL, MAHL had lower aliphatic OH. Longer reaction favored OH oxidation. The aliphatic OH was decreased more than half under M50T100t60 to 1.77 from 3.88 mmol g $^{-1}$ for MWL,[51] consistent with their 2D ^{1}H ^{13}C NMR analysis. No obvious changes in guaiacyl OH were observed, because MA does not directly esterify the phenolic hydroxy group.[106,107] Only under the most severe condition (M50T100t60), did 5-substituted OH in dissolved MAHL show a significant higher level than that in MWL. The small increase in 5-substituted OH in dissolved MAHL from less severe runs (Table 2) strongly suggests a less condensed lignin structure for those runs with a short reaction time of 30 min.[108]

3.3. Comparison AHF using p-TsOH with MAHF

Several aromatic sulfonic acids have hydrotropic properties, as previously stated. Because *p*-TsOH is commercially available in large quantities and has relatively low environmental impact, it was chosen to compare with a dicarboxylic acid hydrotropes, MA.[85] As listed in Table 3, MA is a much weaker acid and less

Table 2. Quantification of functional groups in dissolved MAHL in comparison with MWL by ^{31}P NMR spectroscopy.[51]

Sample	Aliphatic OH [mmol g $^{-1}$]	5-substituted OH [mmol g $^{-1}$]	Guaiacyl OH [mmol g $^{-1}$]	COOH [mmol g $^{-1}$]
MWL	3.88	0.33	0.25	0.12
M60T90t30	3.06	0.53	0.23	0.39
M70T80t30	3.02	0.50	0.21	0.61
M50T100t30	3.24	0.53	0.25	0.45
M50T100t60	1.77	0.90	0.31	0.54

Table 3. Comparison of physical properties between *p*-TsOH and MA.

Property	***p*-TsOH**	**MA**
molecular formula	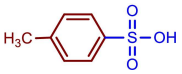	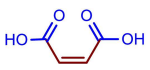
pK_a	2.8	1.9
solubility in water [g L $^{-1}$]	670	479
MHC [wt%]	10.4	25
safety	corrosive to cause skin burns, harmful if swallowed	U.S. FDA-approved indirect food additive (21CFR175-177)

© 2021 The Authors ChemSusChem
© 2021 Chemistry Europe and Wiley-VCH GmbH.
This article has been contributed to by US Government employees and their work is in the public domain in the USA.

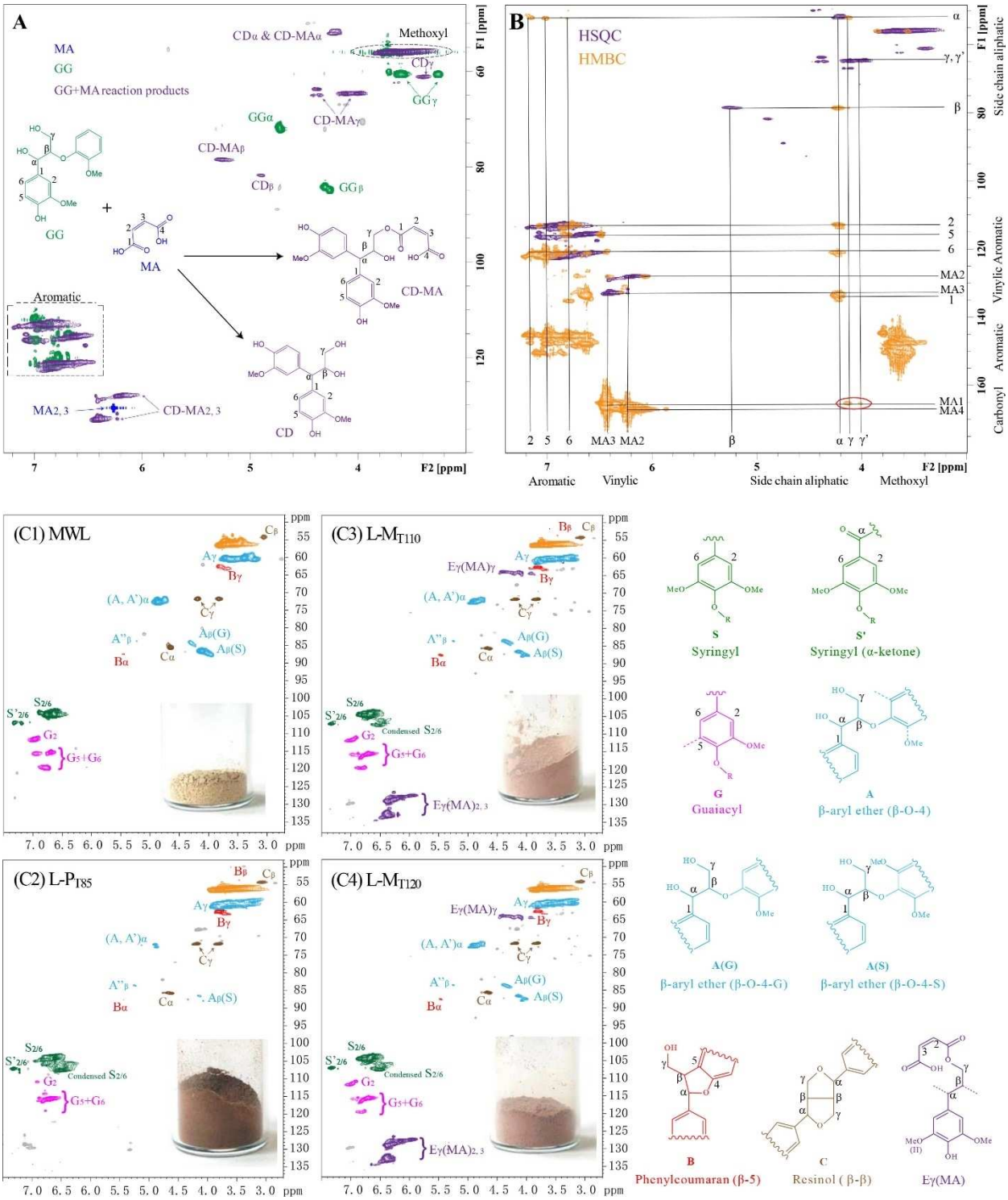

Figure 5. (A) 2D ^{1}H ^{13}C HSQC NMR spectra of MA, GG, and GG-MA. (B) 2D ^{1}H ^{13}C HSQC (purple) and 2D ^{1}H ^{13}C HMBC (orange) spectra of GG-MA. (A,B) reprinted with permission from ref. [51]. Copyright 2020, Royal Society of Chemistry. (C) HQSC spectra of (C1) birch MWL and (C2 C4) MA and *p*-TsOH-dissolved lignin. Reprinted with permission from ref. [85]. Copyright 2020, Wiley-VCH.

corrosive with the first pK_a of 1.9 compared with 2.8 for *p*-TsOH. It also has a lower solubility of 479 g L ^{1} compared with 670 g L ^{1} for *p*-TsOH. MHC is an important property for any hydrotrope. It not only determines the required concentration to solubilize a hydrophobic substance,[53–55] but also determines the amount of water needed for dilution to precipitate/separate the solubilized substance, lignin. As shown in Figure 6A, the conductivity of aqueous *p*-TsOH solution has a distinct

© 2021 The Authors ChemSusChem
© 2021 Chemistry Europe and Wiley-VCH GmbH.
This article has been contributed to by US Government employees and their work is in the public domain in the USA.

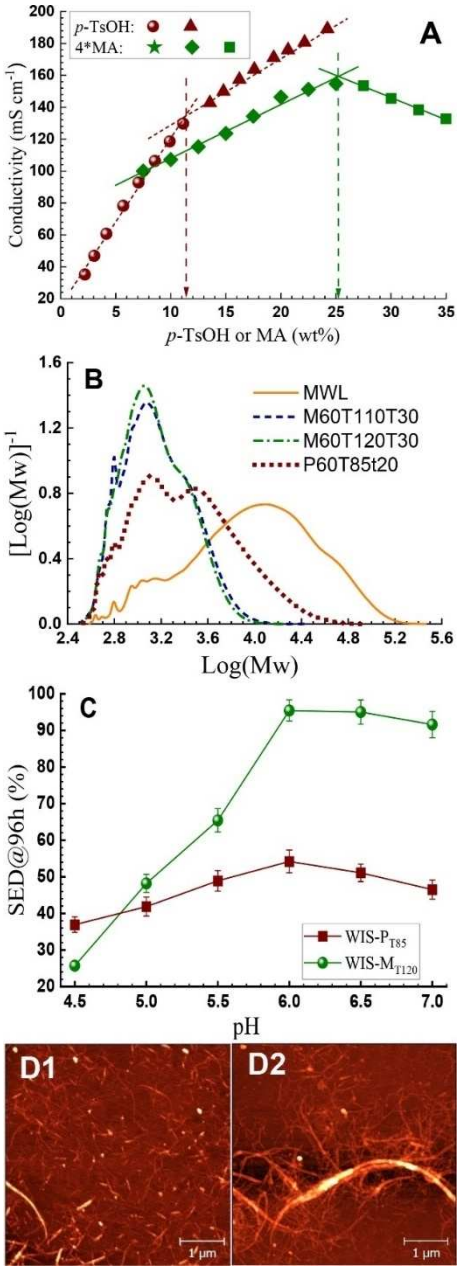

Figure 6. Comparisons of AHF using *p*-TsOH and MAHF for fractionating birch. (A) Minimal hydrotropic concentration. Reprinted with permission from refs. [50,51]. Copyright 2020, Wiley-VCH. (B) Dissolved lignin molecular weight distribution. (C) WIS substrate enzymatic digestibility (SED). (D) LCNFs from (D1) WIS-P_{T85} (D2) and WIS-M_{T120}. (B–D) Reprinted with permission from ref. [85]. Copyright 2020, Wiley-VCH.

transition point. Linear regression of the conductivity using *p*-TsOH concentration as the independent variable resulted in the transition concentration of 11.4 wt%, which is the MHC of *p*-TsOH. This MHC was also verified from DLS-measured lignin particle size as shown in Figure 2A. Similarly, the MHC for MA was determined at 25 wt%. A greater MHC can be advantageous to decrease the amount of dilution water needed for precipitating lignin assuming using the same operating hydrotropic concentration.

To make a meaningful comparison, Cai et al. selected proper conditions including the same acid concentration of 60 wt% to fractionate birch wood so that AHF using *p*-TsOH resulted in approximately the same extent of delignification and xylan (the major hemicellulose in birch) dissolution as those by MAHF.[85] As listed in Table 4, MAHF run M60T120t30 resulted in a very similar WIS yield and composition as those from AHF run M60T85t20 using *p*-TsOH. MAHF Run M60T110t30 was milder. Spectral peaks at δ_C/δ_H = 127.8/6.2, 133.2/6.4, and 63.6/(4.03, 4.39) ppm, which are characteristic of lignin esterification by MA at the γ-OH position,[51] were not observed from the HQSC spectrum of birch wood MWL (Figure 5C1) and AHL, L P_{T85} from P60T85t20 (Figure 5C2), but were clearly shown in the spectra of the two MAHLs, L M_{T110} from M60T110t30 and L M_{T120} from M60T120t230 (Figure 5C3,C4).

Cai et al. also observed significant differences in the molecular weight distributions of the dissolved lignin between the AHL, L P_{T85}, and the two MAHLs (L M_{T110} and L M_{T120}) as shown in Figure 6B.[51] Compared with birch MWL, both AHF and MAHF significantly depolymerized lignin to result in a left shift in lignin molecular weight distribution to the lower molecular weight region. L P_{T85} has two peaks with the higher molecular weight peak due to lignin condensation or repolymerization through the formation of C=C bonds to result in a higher weight averaged M_w of 3300 Da than M_w of approximately 1500 Da for L M_{T110} and L M_{T120} from MAHF (Table 5). Their 2D NMR analyses indicated that the two MAHLs are much less condensed as evidenced by the amount of β-O-4′ linkages retained (Table 5). Lignin condensation was also reflected from the much lighter color of L M_{T110} and L M_{T120} (Figure 5C3,C4) than L P_{T85} (Figure 5C2). Lower lignin condensation resulted in higher yield of monophenols (Table 5)[51] through supercritical methanol dehydration hydrodeoxygenation by catalysis using $CuAlMgO_x$.[109]

Cai et al. demonstrated that lignin carboxylation has significant advantages for enzymatic saccharification of fractionated WIS as well as nanofibrillation of the WIS for producing LCNFs.[51] The fractionated WIS-P_{T85} from P60T85t20 and WIS-M_{T120} from M60T120t30 have very similar chemical composition (Table 4) and therefore resulted in similar SED of approximately 40% at commonly practiced hydrolysis pH ≈ 4.8 as shown in Figure 6C. Using elevated pH = 6.0 in hydrolysis to mediate electrostatic repulsion between substrate lignin and cellulase decreased nonproductive cellulase binding to substrate lignin.[110,111] As a result, SED was increased for both WIS-P_{T85} and WIS-M_{T120} and peaked at pH = 6.0 then decreased.[51] The increase in SED was approximately 140% for WIS-M_{T120} with lignin carboxylation, which was substantially greater than the 35% for WIS-P_{T85} without lignin carboxylation. This is because lignin carboxylation in WIS-M_{T120} increased lignin surface charge, which greatly enhanced electrostatic repulsion between substrate lignin and cellulase, compared with WIS-P_{T85}, which only contained a small amount of native functional hydroxy and carboxyl groups with a lower surface charge even at elevated pH.

To further demonstrate the advantages of MAHF, we compare MAHF with different fractionation processes in

© 2021 The Authors ChemSusChem
© 2021 Chemistry Europe and Wiley-VCH GmbH.
This article has been contributed to by US Government employees and their work is in the public domain in the USA.

Sample[a]	WIS Yield [%]	K. Lignin [%]	Glucan [%]	Xylan [%]	Mannan [%]	Fractionation liquor Xylose [g kg $^{-1}$]	Glucose [g kg $^{-1}$]
birch	–	19.5	40.0	23.0	1.4	–	–
M60T110t30	62.9	16.2	55.2	15.9	1.9	12.4	0.5
		(52.3)	(86.9)	(43.5)	(85.4)	(53.9)	(1.3)
M60T120t30	55.4	12.9	61.3	13.8	1.5	14.9	1.1
		(36.6)	(85.0)	(33.2)	(59.4)	(64.8)	(2.8)
P60T85t20	57.1	12.8	62.9	15.7	2.3	13.6	0.4
		(37.5)	(89.9)	(39.0)	(93.8)	(59.2)	(1.0)

[a] M/P*xx*T*yyy*t*zz*: Mxx or P*xx* stands for Maleic acid or *p*-TsOH concentration at *xx* wt%, T*yyy* stands for temperature at *yyy* °C, t*zz* stands for fractionation time for *zz* min. The numbers in the parentheses are percentages of the component retained in WIS or percentages of wood xylan or mannan converted to xylose or mannose in the fractionated liquor on an untreated dry wood basis.

Table 5. Structural characteristics (interunit linkages, aromatic units, and S/G ratio) of acid hydrotropic dissolved lignin (AHL) from integrating ^{1}H ^{13}C correlation peaks in the HSQC spectra (the condensed $S_{2/6}$ is abbreviated as S_{Cond}).[85]

AHL[a]	S	G	S/G	β-O-4′ [%]	M_n	M_w	M_w/M_n	Monophenols [C%]	C_2 C_5 alcohols yield [C%]
MWL	80.8	19.2	4.2	64.6	3227	14832	4.60	35.9	4.7
L M_{T110}	87.1	12.9	6.7	41.0	1048	1598	1.52	25.8	4.8
L M_{T120}	91.5	8.5	10.7	26.7	1035	1516	1.46	20.2	4.1
L P_{T85}	98.6	1.4	72.5	3.6	1346	3290	2.44	16.9	3.3

[a] L M_{T110} and L M_{T120}: by maleic acid at 110 and 120 °C for 30 min, respectively; L $P_{T85:}$ by *p*-TsOH at 85 °C for 20 min.

enzymatic saccharification of fractionated cellulosic WIS. As listed in Table 6, data from poplar wood again shows that AHF using *p*-TsOH underperforms MAHF. AHF with *p*-TsOH[50] also underperformed SPORL(Sulfite Pretreatment to Overcome the Recalcitrance of Lignocelluloses).[112] Only with significantly more dissolutions of xylan and lignin under higher temperatures did organosolv processes[113,114] achieve better SED than did MAHF.[51] The data from wheat straw clearly shows that MAHF performed significantly better than high temperature hydrothermal, dilute acid, IL, and DES fractionation processes. With additional bleaching to remove approximately 95% lignin and 40% more cellulase, dilute acid treatment[115] achieved similar SED (90%) to that of MAHF. The very long reaction time of several hours required for effective fractionation using the DES system is a significant disadvantage. A recent study indicated that using *p*-TsOH as an H-bonding donor to form a DES system with ChCl was able to substantially decrease reaction time to 20 min to achieve approximately 90% delignification at 80 °C.[116] It is possible that *p*-TsOH may also have played a hydrotrope role in solubilizing lignin in addition to being the H-bonding donor.

Lignin carboxylation also enhanced the lignin lubrication effect[121,122] in fibrillating lignocelluloses for producing LCNFs as demonstrated by Cai et al.[51] Both WIS-P_{T85} and WIS-M_{T120} can be easily fibrillated into LCNFs with just one pass through microfluidization. Despite these two WIS having very similar extent of delignification and hemicelluloses dissolution (Table 4), the LCNFs from WIS-M_{T120} had a much thinner (Figure 6D1) and narrower diameter distribution (peaked at 12 nm) than those from WIS-P_{T85} with a thicker (Figure 6D2) and broader distribution (peaked at 23 nm). Carboxylation of lignin in WIS was verified by conductometric titration of the LCNFs from three passes through microfluidization with carboxyl group content of 0.22 and 0.06 mmol g $^{-1}$ for the LCNF samples from WIS-M_{T120} and WIS-P_{T85}, respectively.[51] The carboxylated LCNFs with surface charge more than 40 mV can facilitate dispersion. Later, carboxylation (esterification) of residue lignin (RL) in WIS was also verified by 2D NMR analyses in switchgrass[123] and wheat straw.[124]

3.4. Bleaching water insoluble cellulosic solids from AHF

It is known that lignocellulosic fibers containing less condensed lignin structure are easier to bleach.[125,126] Ma et al. demonstrated that AHF birch wood fibers fractionated using *p*-TsOH with a greater amount of β-O-4′ linkages are much easier to bleach than fibers with a similar level of delignification but containing less β-O-4′ bonds.[66] They found that less condensed lignin greatly facilitated oxidative bleaching such as oxygen and peroxide bleaching. Using *p*-TsOH at 60 wt% and 90 °C, a batch AHF for 30 min resulted in a WIS, *p*Ba-t30, with a higher lignin content of 7.1% (pulp kappa number: $\kappa = 40$). Washing with *p*-TsOH three times decreased lignin content to 3.7% ($\kappa = 20$) for the washed WIS *p*Ba-t30W3, higher than the value of 4.7% ($\kappa = 24$) for the WIS from flow-through AHF at the same *p*-TsOH concentration and temperature but for 20 min and washed with water only, *p*FT-t20. However, the lignin in *p*FT-t20 was less condensed due to a shorter reaction time with a greater amount of β-O-4′ linkages of 16% than the 7% that *p*Ba-t30W3 had. As shown in Figure 7, *p*FT-t20 resulted in a higher brightness and lower κ number than both *p*Ba-t30 and *p*Ba-t30W3 after one stage oxygen bleaching. Similar results were also obtained for fibers from MAHF. Higher brightness and

© 2021 The Authors ChemSusChem
© 2021 Chemistry Europe and Wiley-VCH GmbH.
This article has been contributed to by US Government employees and their work is in the public domain in the USA.

Method	Biomass	Fractionation condition	Xylan; lignin removal [%]	Enzyme loading[a]	SED [%]	Ref.
MAHF	poplar fibers	MA = 50 wt% T = 100 °C; t = 60 min	70; 49	CTec3 = 10 6 FPU(g solids) $^{-1}$	89 ± 3	[51]
AHF (*p*-TsOH)	poplar fibers	*p*-TsOH = 50 wt% T = 90 °C; t = 112 min	80; 84	CTec3 = 20	93 ± 2	[67]
AHF (*p*-TsOH)	poplar fibers	*p*-TsOH = 75 wt% T = 80 °C; t = 20 min	81; 86	CTec3 = 10 CTec3 = 20	59 87	[50]
dilute acid SPORL	poplar chips	T = 160 °C; t = 58 min H_2SO_4 = 2 mL L^{-1} +$NaHSO_3$ = 0 % +$NaHSO_3$ = 1.3 %	78; 3 84; 31	CTec3 = 10 CTec3 = 10	52 80	[112]
MAHF AHF (*p*-TsOH)	birch fibers	MA = 60 wt%; t = 30 min T = 110 °C T = 120 °C *p*-TsOH = 60 wt% T = 85 °C; t = 20 min	58; 48 67; 63 61; 63	CTec3 = 10 CTec3 = 10 CTec3 = 7.5 CTec3 = 5 CTec3 = 10	85 98 90 71 54	[51]
acetone organosolv	birch particles (2 mm)	acetone = 50 wt% +H_2SO_4 = 3.9 g L^{-1} T = 140 °C; t = 120 min	92; 86	Accelerase TRIO = 14 10 FPU (g solids) $^{-1}$	≈90	[113]
alkaline oxidation/steam explosion	birch chips	Na_2CO_3 = 26.5 g L^{-1} T = 120 °C; t = 1200 min steam H_2SO_4 = 5 g L^{-1} T = 200 °C; t = 5 min	≈100; NA ≈100; NA	Celluclast 1.5 L = 10 FPU(g solids) $^{-1}$ +Novozymes 188	≈95 ≈95	[117]
organosolv	birch residue	SO_2 + ethanol + H_2O (12 + 44 + 44) wt % T = 150 °C; t = 30 min	80; 93	CTec2 = 8	≈95	[114]
MAHF	wheat straw hammer milled (8 mm long)	MA = 40 wt% T = 80 °C; t = 120 min MA = 60 wt% T = 100 °C; t = 30 min MA = 60 wt% T = 120 °C; t = 60 min	66; 38 67; 54 76; 57	CTec3 = 10	42 78 89	[124]
steam explosion	wheat straw	T = 190 °C; t = 10 min	86; ≈0	CTec2 (+LPMO) = 10	77	[118]
dilute acid/dilute acid +bleaching	wheat straw 20–40 mesh	T = 120 °C; t = 60 min H_2SO_4 = 1 % H_2SO_4 = 3 % H_2SO_4 = 1 % + $NaClO_2$ T = 75 °C; t = 180 min	71; 5 86; 2 77; 94	CTec2 = 20 CTec2 = 18 CTec2 = 14	44 46 90	[115]
IL	wheat straw	[emin][HSO_4] = 41.3 wt % 131 °C; 88 min (< 0. 5 mm knife-milled)	80; ≈0	CTec2 ≈ 20	76	[119]
DES	wheat straw 60 mesh	TEBAC/LA (1 : 9) T = 100 °C; 10 h	≈73; ≈73	Celluclast 1.5 L = 35 FPU(g solids) $^{-1}$ +β-glucosidase = 82 CBU(g solids) $^{-1}$	89	[120]

[a] Unit in FPU (g glucan) $^{-1}$ unless indicated.

higher fiber yield were obtained from bleaching fibers with higher lignin content produced from a less severe MAHF run with lower extent of lignin condensation or higher β-O-4′ linkages than fibers from a more severe fraction with a lower initial lignin content.[123]

3.5. Kinetic analyses of AHF and MAHF

Reaction kinetics based severities such as combined hydrolysis factor (CHF)[127] and combined delignification factor (CDF)[68] have been applied to predict hemicellulose dissolution and delignification in AHF using *p*-TsOH and MAHF,[67,90,123,128] respectively. As shown in Equations (1a), (1b) and (2a), (2b), the amount of xylan and lignin retained, X_R and L_R, can be expressed as a single independent variable function of CHF and CDF, respectively:

$$X_R = (1 \quad \theta \quad \theta_R)e^{\ \mathrm{CHF}} + \theta \times e^{\ f\times\mathrm{CHF}} + \theta_R \tag{1a}$$

$$\mathrm{CHF} = \boldsymbol{exp}(\alpha \quad \frac{E}{\boldsymbol{RT}} + \beta\boldsymbol{C}\ ) \times C \times t \tag{1b}$$

$$L_R = (1 \quad \theta' \quad \theta'_R)e^{\ \mathrm{CDF}} + \theta' \times e^{\ f'\times\mathrm{CDF}} + \theta'_R \tag{2a}$$

© 2021 The Authors ChemSusChem
© 2021 Chemistry Europe and Wiley-VCH GmbH.
This article has been contributed to by US Government employees and their work is in the public domain in the USA.

Figure 7. Effect of lignin condensation on oxygen bleaching of WIS from AHF using *p*-TsOH at 60 wt% and 90 °C. Top row: unbleached WISs. Bottom row: oxygen-bleached WISs at O_2 pressure of 0.75 MPa, NaOH charge of 6% on WIS, and 110 °C for 60 min. Left column: water-washed WIS *p*Ba-t30 from batch AHF for 30 min. Middle column: *p*Ba-t30 washed with *p*-TsOH three times. Right column: only water-washed WIS *p*FT-t20 from flow-through AHF for 20 min. Reprinted with permission from ref. [66]. Copyright 2020, American Chemical Society.

$$\mathrm{CDF} = \boldsymbol{exp}(\alpha' \quad \frac{E'^{\leftarrow}}{RT} + \beta' C) \times C \times t \qquad (2b)$$

where C is the acid hydrotrope molar concentration [mol L ^{1}], R=8.314 J mol ^{1}K ^{1} is the universal gas content, t is reaction time [min], and T is reaction temperature [K]. α, α', and β, β' are adjustable parameters, E and E' are apparent activation energies [J mol ^{1}], and θ and θ' are the initial fraction of slow-reacting xylan and lignin, respectively. f and f' are the ratios of reaction rates between slow and fast xylan and slow and fast lignin, respectively. θ_R and θ_R' are residual xylan and lignin, respectively. All parameters in Equations (1a), (1b) and (2a), (2b) can be obtained by fitting experimentally measured xylan and lignin dissolution data.

The significance of this type of kinetic analysis is for process scale-up. For example, as long as the same CDF is maintained, the same amount of delignification can be achieved in the scale-up facility without using the identical individual fractionation conditions identified in lab scale to provide scale-up flexibility and avoid facility constraints in scale-up facilities. For example, a low acid concentration can be used in scale-up runs to decrease acid recovery capacity by slightly increasing temperature or reaction time to achieve the same desired fractionation results.

3.6. Recycling and reuse of acid hydrotrope and furfural production

Chen et al. demonstrated the reusability of *p*-TsOH spent liquor from AHF under P70T65t20 in subsequent runs under the same condition using the same amount of poplar wood.[50] The spent liquor was collected from solid-liquor separation right after fractionation. They calculated the amount of fresh makeup *p*-TsOH solution needed for the subsequent cycles based on the difference between the fresh liquor volume in the first run and the amount of spent liquor collected. They found negligible differences in the chemical compositions between the fractionated poplar wood WIS from the first run using fresh liquor and the WISs from the subsequent three runs using recycled spent liquors. Cai et al. collected the spent liquor from MAHF under M50T100t30 along with the first washing filtrate diluted to MA concentration of 15% to precipitate lignin.[51] They extracted remaining colloidal lignin particles using n-pentanol. They then dehydrated the diluted and lignin-removed spent liquor using batch distillation. They obtained a furfural yield of approximately 70% from the dissolved xylose. The dehydrated spent liquor at approximately 50 wt% concentration was reused for subsequent fractionation under the same condition. With the spiking of 5% fresh MA to compensate losses in each reuse cycle, they found negligible differences in the chemical compositions between the fractionated poplar wood WIS from the first MAHF run using fresh aqueous MA solution and the WISs from the subsequent two runs using recycled spent liquors, suggesting a MA recovery of 95% was achieved.[51]

Quantifications of the absolute amounts of recoverable acid hydrotrope and lignin were also carried out. Cheng et al. quantified the amounts of *p*-TsOH in the collected spent liquor and subsequent four washing filtrates from different fractionation conditions.[90] They found that the amounts of *p*-TsOH in the third washing filtrate from all runs were negligible; furthermore, the *p*-TsOH loss was less than 2% through collecting the spent liquor and the filtrates from the first three washings. Cai et al. compared the amount of acid hydrotrope recoverable from AHF using *p*-TsOH and MAHF after lignin removal through dilution and resin extraction and distillation of dissolved xylose as shown in Figure 8.[51] During their experiments under P60T85t20 and M60T120t30, they only measured the amounts of hydrotrope in the collected spent liquor and first washing filtrate diluted to 10 and 20 wt% acid concentration for AHF and MAHF, respectively. They found the absolute amounts of *p*-TsOH and MA recovered were 87 and

Figure 8. The fractionated liquor (60 wt%) was diluted to different acid concentrations (30, 20, 10, 5 wt%) to precipitate lignin, and after centrifugation, the residual lignin in the supernatant was adsorbed by resin and the solid acid was recovered by evaporation and cooling crystallization. Reprinted with permission from ref. [85]. Copyright 2020, Wiley-VCH.

© 2021 The Authors ChemSusChem
© 2021 Chemistry Europe and Wiley-VCH GmbH.
This article has been contributed to by US Government employees and their work is in the public domain in the USA.

76% with purities of 96 and 94%, respectively. The amount of collectable lignin from water dilution alone was more than 80% for both runs.

4. Future Perspectives and Closing Remarks

4.1. Improving understanding of the lignin solubilization mechanism

Lignin solubilization is crucial in biomass fractionation. Understanding its mechanism could tailor efficient and sustainable fractionation. Activation energies for chemical bond cleavages can be used as a guide to understanding lignin dissolution. The activation energies of diverse linkages have been computationally and experimentally investigated. The reported activation energies of approximately 19 kcal mol ^{1} for lignin-carbohydrate complex (LCC) cleavages were substantially higher than approximately 11 kcal mol ^{1} for Cβ-O-4′ cleavages and 3 kcal mol ^{1} for Cα OH dehydration under acidic environments.[129] Therefore, the cleavage of Cβ-O-4′ and dehydration of Cα OH bonding of lignin is unavoidable in order to break the LCCs using harsh reaction conditions. From a lignin valorization point of view, preserving Cβ-O-4′ linkages is critical for further processing from depolymerization to aromatics or using lignin as a polymer with low glass transition temperature to facilitate compounding. Preserving Cα OH bonding can prevent the formation of benzylic carbocation that is readily condensable through forming recalcitrant C C bonding products. Some strategies have been proposed to preserve the Cβ-O-4′ linkages, for example, using biocatalysts including cellulase and xylanase to selectively diminish the active energies for depolymerizing cellulose and hemicelluloses,[130,131] respectively. However, the high cost and low efficiency of enzymatic reactions limited scale-up. Concentrated acids were also found to decrease the activation energies by disrupting the hydrogen bonding in the biomass matrix and improving the reaction homogeneity, but concentrated acids showed no selectivity at low-temperature and pressure conditions.[129,132] It appears that flow-through technique or "good" solvents extraction can be synergistically carried out to prevent lignin condensation. In the future, chemistry on selectively and efficiently cleaving LCCs should be developed so that lignocellulose fractionization can be carried out under mild conditions. Recently, studies mainly focused on the stabilization of reactive intermediates from reductive catalytic fractionation, oxidation, or functionalization.[129] However, each stabilization strategy has its own limitations. Their potential synergistic effects and mechanisms should be investigated. More importantly, the utility of different fractions of fractionated lignocelluloses, especially the carbohydrate fraction with approximately 60% of the lignocelluloses, and the recyclability of any chemicals involved should be considered.

4.2. Selection of new acid hydrotropes

Apparently, the selected concentrated acid hydrotrope solution should firstly be strong enough to break LCCs and decrease the activation energies of lignocelluloses so that fractionation can be carried out at a low temperature and pressure while inhibiting lignin repolymerization. Secondly, the acid hydrotropes should have a suitable apolarity moiety to produce optimum aggregation around isolated/separated lignin.[55] It is known that lignin repolymerization is inevitable in acidic fractionation including acid hydrotropic fractionation (AHF) and maleic acid hydrotropic fractionation (MAHF). Therefore, choosing acid hydrotropes capable of stabilizing the fractionated reactive intermediates through functionalization will be ideal. For example, MA can prevent lignin from condensation by esterification due to electrostatic repulsive force between the carboxylated lignin molecules to decrease their contact. Of course, functionalization should take the downstream valorization into account. From the chemical loading and water usage point of view, acid hydrotropes with a low effective concentration and a high minimum hydrotrope concentration (MHC), or a steep sigmoidal solubility curve, can decrease hydrotrope loading while decreasing water usage for dilution to precipitate lignin. In this sense, MA with a MHC of 25 wt% is better than *p*-TsOH with MHC of 10 wt%. Finally, the acid hydrotropes should have low toxicity and good recyclability and reusability. MA as a U.S. FDA-approved indirect food additive (21CFR175-177) and has significant advantages in terms of environmental sustainability and applications of fractionated cellulosic fibers related to food and food packaging.

4.3. Process integration and commercialization

The results presented in this Minireview suggest that the superior fractionation performance of AHF and especially MAHF is undisputable in comparison with ionic liquids, deep eutectic solvents, and other cosolvent systems. However, like any solvent system, the commercial success of AHF or MAHF is heavily dependent on efficient lignin separation, dissolved sugar separation and conversion, and acid recovery. Existing work has demonstrated the potential pathways to address these critical issues. Improving process integration by improving furfural yield and titer and inhibiting undesirable reactions that lead to the formation of humic substances[133] is a high-value proposition and can be learned from existing furfural production technologies. Membrane separation technologies that can directly separate acid hydrotrope from dissolved sugars and water should also be explored for producing other high-value chemicals other than furfural from dissolved sugars and to decrease water evaporation. It appears that the fractionated cellulosic solid fraction can be directly used to produced lignin-containing cellulose nanofibrils, a high-value material that still needs to find a commercial market. With a high extent of delignification and bleaching, it appears that the cellulosic fractionation is suitable for dissolving pulp fibers, which needs

© 2021 The Authors ChemSusChem
© 2021 Chemistry Europe and Wiley-VCH GmbH.
This article has been contributed to by US Government employees and their work is in the public domain in the USA.

to be further evaluated. The cellulosic fraction can also be used for enzymatic sugar production and MAHF is better suited because of lignin carboxylation decreased nonproductive cellulase binding an elevated pH.[85,110] Optimizations are needed with focus on decreasing acid loading while achieving a good degree of carboxylation. The carboxylated MAHL with good dispersibility can be used as a rheology modifier in coatings and paints and possibly cosmetics. These potentially immediate applications in various commercial markets should be evaluated. The substantial amount of progress and developed technologies in lignin valorization through depolymerization or use as polymers can be directly tapped for AHF and MAHF.

Keywords: acid hydrotropic fractionation · biorefinery · cellulosic materials · lignin valorization · lignocellulose

[1] R. D. Perlack, B. J. Stokes, *Oak Ridge Natl. Lab. [Rep.] ORNL-TM* **2011**, *2011/224*.
[2] P. Zhang, T. Wei, Z. Jia, Q. Han, X. Ren, Y. Li, *PLoS One* **2014**, *9*.
[3] W. Xie, Y. Zhang, T. Wu, *Soil Tillage Res.* **2017**, *169*, 1–6.
[4] J. Clark, F. Deswarte, *Introduction to Chemicals from Biomass*, Wiley, **2015**.
[5] H. Kopetz, *Nature* **2013**, *494*, 29–31.
[6] J. J. Bozell, G. R. Petersen, *Green Chem.* **2010**, *12*, 539–554.
[7] J. Y. Zhu, X. J. Pan, G. S. Wang, R. Gleisner, *Bioresour. Technol.* **2009**, *100*, 2411–2418.
[8] Y. L. Zhao, Y. Wang, J. Y. Zhu, A. Ragauskas, Y. L. Deng, *Biotechnol. Bioeng.* **2008**, *99*, 1320–1328.
[9] J. S. Kim, Y. Y. Lee, T. H. Kim, *Bioresour. Technol.* **2016**, *199*, 42–48.
[10] E. E. Harris, E. Beglinger, *Ind. Eng. Chem.* **1946**, *38*, 890–895.
[11] J. W. Lee, C. J. Houtman, H. Y. Kim, I. G. Choi, T. W. Jeffries, *Bioresour. Technol.* **2011**, *102*, 7451–7456.
[12] S. M. Ewanick, R. Bura, J. N. Saddler, *Biotechnol. Bioeng.* **2007**, *98*, 737–746.
[13] I. De Bari, F. Nanna, G. Braccio, *Ind. Eng. Chem. Res.* **2007**, *46*, 7711–7720.
[14] C. Tengborg, K. Stenberg, M. Galbe, G. Zacchi, S. Larsson, E. Palmqvist, B. Hahn-Hägerdal, *Appl. Biochem. Biotechnol.* **1998**, *70–72*, 3–15.
[15] V. Balan, L. da Costa Sousa, S. P. S. Chundawat, D. Marshall, L. N. Sharma, C. K. Chambliss, B. E. Dale, *Biotechnol. Prog.* **2009**, *25*, 365–375.
[16] T. H. Kim, J. S. Kim, C. Sunwoo, Y. Y. Lee, *Bioresour. Technol.* **2003**, *90*, 39–47.
[17] X. Pan, N. Gilkes, J. Kadla, K. Pye, S. Saka, D. Gregg, K. Ehara, D. Xie, D. Lam, J. Saddler, *Biotechnol. Bioeng.* **2006**, *94*, 851–861.
[18] M. Iakovlev, A. van Heiningen, *ChemSusChem* **2012**, *5*, 1625–1637.
[19] X. Zhao, D. Liu, *Bioresour. Technol.* **2012**, *117*, 25–32.
[20] G. Gellerstedt, E. L. Lindfors, *Holzforschung* **1984**, *38*, 151–158.
[21] R. Rinaldi, R. Jastrzebski, M. T. Clough, J. Ralph, M. Kennema, P. C. A. Bruijnincx, B. M. Weckhuysen, *Angew. Chem. Int. Ed.* **2016**, *55*, 8164–8215; *Angew. Chem.* **2016**, *128*, 8296–8354.
[22] P. J. Deuss, C. S. Lancefield, A. Narani, J. G. De Vries, N. J. Westwood, K. Barta, *Green Chem.* **2017**, *19*, 2774–2782.
[23] M. V. Galkin, J. S. M. Samec, *ChemSusChem* **2016**, *9*, 1544–1558.
[24] J. S. Luterbacher, J. M. Rand, D. M. Alonso, J. Han, J. T. Youngquist, C. T. Maravelias, B. F. Pfleger, J. A. Dumesic, *Sci. J.* **2014**, *343*, 277–280.
[25] C. M. Cai, T. Zhang, R. Kumar, C. E. Wyman, *Green Chem.* **2013**, *15*, 3140–3145.
[26] I. Anugwom, V. Eta, P. Virtanen, P. Mäki-Arvela, M. Hedenström, M. Hummel, H. Sixta, J. P. Mikkola, *ChemSusChem* **2014**, *7*, 1170–1176.
[27] A. Brandt, J. Gräsvik, J. P. Hallett, T. Welton, *Green Chem.* **2013**, *15*, 550–583.
[28] A. M. Socha, R. Parthasarathi, J. Shi, S. Pattathil, D. Whyte, M. Bergeron, A. George, K. Tran, V. Stavila, S. Venkatachalam, M. G. Hahn, B. A. Simmons, S. Singh, *Proc. Natl. Acad. Sci. USA* **2014**, *111*, E3587–E3595.
[29] M. Chen, F. Malaret, A. E. J. Firth, P. Verdía, A. R. Abouelela, Y. Chen, J. P. Hallett, *Green Chem.* **2020**, *22*, 5161–5178.
[30] J. T. Gorke, F. Srienc, R. J. Kazlauskas, *Chem. Commun.* **2008**, 1235–1237.
[31] X. Tang, M. Zuo, Z. Li, H. Liu, C. Xiong, X. Zeng, Y. Sun, L. Hu, S. Liu, T. Lei, L. Lin, *ChemSusChem.* **2017**, *10*, 2695.
[32] Y. Liu, B. Guo, Q. Xia, J. Meng, W. Chen, S. Liu, Q. Wang, J. Li, H. Yu, *ACS Sustainable Chem. Eng.* **2017**, *5*, 7623–7631.
[33] C. Alvarez-Vasco, R. Ma, M. Quintero, M. Guo, S. Geleynse, K. K. Ramasamy, M. Wolcott, X. Zhang, *Green Chem.* **2016**, *18*, 5133–5141.
[34] Y. Y. Wang, P. Sengupta, B. Scheidemantle, Y. Pu, C. E. Wyman, C. M. Cai, A. J. Ragauskas, *Front. Energy Res.* **2020**, *8*, 149, DOI: 10.3389/fenrg.2020.00149.
[35] F. J. V. Gschwend, C. L. Chambon, M. Biedka, A. Brandt-Talbot, P. S. Fennell, J. P. Hallett, *Green Chem.* **2019**, *21*, 692–703.
[36] T. P. Thuy Pham, C. W. Cho, Y. S. Yun, *Water Res.* **2010**, *44*, 352–372.
[37] Q. Wen, J. X. Chen, Y. L. Tang, J. Wang, Z. Yang, *Chemosphere* **2015**, *132*, 63–69.
[38] J. Fowles, R. Boatman, J. Bootman, C. Lewis, D. Morgott, E. Rushton, J. Van Rooij, M. Banton, *Crit. Rev. Toxicol.* **2013**, *43*, 811–828.
[39] EPA, *US Environmental Protection Agency CAS No. 109-99-9.* **2012**, *EPA/635/R-11/006F*, www.epa.gov/iris.
[40] S. Van Den Bosch, W. Schutyser, R. Vanholme, T. Driessen, S. F. Koelewijn, T. Renders, B. De Meester, W. J. J. Huijgen, W. Dehaen, C. M. Courtin, B. Lagrain, W. Boerjan, B. F. Sels, *Energy Environ. Sci.* **2015**, *8*, 1748–1763.
[41] Z. Sun, B. Fridrich, A. De Santi, S. Elangovan, K. Barta, *Chem. Rev.* **2018**, *118*, 614–678.
[42] S. Wang, L. Shuai, B. Saha, D. G. Vlachos, T. H. Epps, *ACS Cent. Sci.* **2018**, *4*, 701–708.
[43] P. Ferrini, R. Rinaldi, *Angew. Chem. Int. Ed.* **2014**, *53*, 8634–8639; *Angew. Chem.* **2014**, *126*, 8778–8783.
[44] T. Parsell, S. Yohe, J. Degenstein, T. Jarrell, I. Klein, E. Gencer, B. Hewetson, M. Hurt, J. I. Kim, H. Choudhari, B. Saha, R. Meilan, N. Mosier, F. Ribeiro, W. N. Delgass, C. Chapple, H. I. Kenttämaa, R. Agrawal, M. M. Abu-Omar, *Green Chem.* **2015**, *17*, 1492–1499.
[45] E. M. Anderson, R. Katahira, M. Reed, M. G. Resch, E. M. Karp, G. T. Beckham, Y. Román-Leshkov, *ACS Sustainable Chem. Eng.* **2016**, *4*, 6940–6950.
[46] I. Kumaniaev, E. Subbotina, J. Sävmarker, M. Larhed, M. V. Galkin, J. S. M. Samec, *Green Chem.* **2017**, *19*, 5767–5771.
[47] M. V. Galkin, A. T. Smit, E. Subbotina, K. A. Artemenko, J. Bergquist, W. J. J. Huijgen, J. S. M. Samec, *ChemSusChem* **2016**, *9*, 3280–3287.
[48] Z. Sun, G. Bottari, A. Afanasenko, M. C. A. Stuart, P. J. Deuss, B. Fridrich, K. Barta, *Nat. Catal.* **2018**, *1*, 82–92.
[49] Z. Wang, S. Qiu, K. Hirth, J. Cheng, J. Wen, N. Li, Y. Fang, X. Pan, J. Y. Zhu, *ACS Sustainable Chem. Eng.* **2019**, *7*, 10808–10820.
[50] L. Chen, J. Dou, Q. Ma, N. Li, R. Wu, H. Bian, D. J. Yelle, T. Vuorinen, S. Fu, X. Pan, J. Y. Zhu, *Sci. Adv.* **2017**, *3*, e1701735.
[51] C. Cai, K. Hirth, R. Gleisner, H. Lou, X. Qiu, J. Y. Zhu, *Green Chem.* **2020**, *22*, 1605–1617.
[52] C. Neuberg, *Biochem. Z.* **1916**, *76*, 106.
[53] J. Eastoe, M. H. Hatzopoulos, P. J. Dowding, *Soft Matter.* **2011**, *7*, 5917–5925.
[54] S. Das, S. Paul, *J. Phys. Chem. B* **2016**, *120*, 173–183.
[55] D. O. Abranches, J. Benfica, B. P. Soares, A. Leal-Duaso, T. E. Sintra, E. Pires, S. P. Pinho, S. Shimizu, J. A. P. Coutinho, *Chem. Commun.* **2020**, *56*, 7143–7146.
[56] V. Dhapte, P. Mehta, *St. Petersburg Polytech. Univ. J.: Phys. Math.* **2015**, *1*, 424–435.
[57] W. Kunz, K. Holmberg, T. Zemb, *Curr. Opin. Colloid Interface Sci.* **2016**, *22*, 99–107.
[58] J. Mehringer, T.-M. Do, D. Touraud, M. Hohenschutz, A. Khoshsima, D. Horinek, W. Kunz, *Cell Rep. Phys. Sci.* **2021**, *2*, 100343.
[59] M. Hopkins Hatzopoulos, J. Eastoe, P. J. Dowding, S. E. Rogers, R. Heenan, R. Dyer, *Langmuir* **2011**, *27*, 12346–12353.
[60] G. Salvi, P. De Los Rios, M. Vendruscolo, *Proteins Struct. Funct. Bioinf.* **2005**, *61*, 492–499.
[61] J. Mehringer, E. Hofmann, D. Touraud, S. Koltzenburg, M. Kellermeier, W. Kunz, *Phys. Chem. Chem. Phys.* **2021**, *23*, 1381–1391.
[62] N. J. Buurma, *Curr. Opin. Colloid Interface Sci.* **2017**, *32*, 69–75.
[63] T. Buchecker, S. Krickl, R. Winkler, I. Grillo, P. Bauduin, D. Touraud, A. Pfitzner, W. Kunz, *Phys. Chem. Chem. Phys.* **2017**, *19*, 1806–1816.
[64] S. Shimizu, N. Matubayasi, *Phys. Chem. Chem. Phys.* **2016**, *18*, 25621–25628.

© 2021 The Authors ChemSusChem
© 2021 Chemistry Europe and Wiley-VCH GmbH.
This article has been contributed to by US Government employees and their work is in the public domain in the USA.

[65] B. P. Soares, D. O. Abranches, T. E. Sintra, A. Leal-Duaso, J. I. García, E. Pires, S. Shimizu, S. P. Pinho, J. A. P. Coutinho, *ACS Sustainable Chem. Eng.* **2020**, *8*, 5742–5749.
[66] Q. Ma, K. Hirth, H. Zhai, J. Y. Zhu, *ACS Sustainable Chem. Eng.* **2020**, *8*, 9046–9057.
[67] J. Zhu, L. Chen, R. Gleisner, J. Y. Zhu, *Fuel* **2019**, *254*, 115572.
[68] Q. Ma, J. Zhu, R. Gleisner, R. Yang, J. Y. Zhu, *ACS Sustainable Chem. Eng.* **2018**, *6*, 14480–14489.
[69] J. Dou, H. Bian, D. J. Yelle, M. Ago, K. Vajanto, T. Vuorinen, J. Y. Zhu, *Ind. Crops Prod.* **2019**, *129*, 15–23.
[70] H. Ji, P. Lv, *Green Chem.* **2020**, *22*, 1378–1387.
[71] L. Chen, X. Zhou, Y. Shi, B. Gao, J. Wu, T. B. Kirk, J. Xu, W. Xue, *Chem. Eng. J.* **2018**, *346*, 217–225.
[72] D. He, Y. Wang, C. G. Yoo, Q.-J. Chen, Q. Yang, *Green Chem.* **2020**, *22*, 5414–5422.
[73] M. G. Neumann, C. C. Schmitt, K. R. Prieto, B. E. Goi, *J. Colloid Interface Sci.* **2007**, *315*, 810–813.
[74] D. Tarasov, M. Leitch, P. Fatehi, *Biotechnol. Biofuels* **2018**, *11*, 269.
[75] N. Giummarella, Y. Pu, A. J. Ragauskas, M. Lawoko, *Green Chem.* **2019**, *21*, 1573–1595.
[76] H. Nishimura, A. Kamiya, T. Nagata, M. Katahira, T. Watanabe, *Sci. Rep.* **2018**, *8*, 6538.
[77] M. Busse-Wicher, T. C. F. Gomes, T. Tryfona, N. Nikolovski, K. Stott, N. J. Grantham, D. N. Bolam, M. S. Skaf, P. Dupree, *Plant J.* **2014**, *79*, 492–506.
[78] X. Kang, A. Kirui, M. C. Dickwella Widanage, F. Mentink-Vigier, D. J. Cosgrove, T. Wang, *Nat. Commun.* **2019**, *10*, 347.
[79] O. M. Terrett, J. J. Lyczakowski, L. Yu, D. Iuga, W. T. Franks, S. P. Brown, R. Dupree, P. Dupree, *Nat. Commun.* **2019**, *10*, 4978.
[80] R. H. McKee, US Patent 2308564, **1943**.
[81] A. R. Procter, *Pulp Pap. Mag. Can.* **1971**, *72*, 67–74.
[82] H. Y. Mou, E. Heikkilä, P. Fardim, *Bioresour. Technol.* **2013**, *150*, 36–41.
[83] K. Gabov, R. J. A. Gosselink, A. I. Smeds, P. Fardim, *J. Agric. Food Chem.* **2014**, *62*, 10759–10767.
[84] H. Mou, P. Fardim, S. Wu in *Biomass Fractionation Technologies for a Lignocellulosic Feedstock Based Biorefinery* (Ed: S. I. Mussatto), **2016**, Chap. 13, pp. 281–313.
[85] C. Cai, J. Li, K. Hirth, G. W. Huber, H. Lou, J. Y. Zhu, *ChemSusChem* **2020**, *13*, 4649–4659.
[86] Q. Ma, L. Chen, W. Wang, R. Yang, J. Y. Zhu, *Holzforschung* **2018**, *72*, 933–942.
[87] J. Y. Zhu, U. P. Agarwal, P. N. Ciesielski, M. E. Himmel, R. Gao, Y. Deng, M. Morits, M. Österberg, *Biotechnol. Biofuels* **2021**, *14*, 114.
[88] H. Bian, L. Chen, R. Gleisner, H. Dai, J. Y. Zhu, *Green Chem.* **2017**, *19*, 3370–3379.
[89] W. Wang, M. D. Mozuch, R. C. Sabo, P. Kersten, J. Y. Zhu, Y. Jin, *Cellulose* **2015**, *22*, 351–361.
[90] J. Cheng, K. Hirth, Q. Ma, J. Zhu, Z. Wang, J. Y. Zhu, *Ind. Eng. Chem. Res.* **2019**, *58*, 7063–7073.
[91] S. Constant, H. L. J. Wienk, A. E. Frissen, P. D. Peinder, R. Boelens, D. S. Van Es, R. J. H. Grisel, B. M. Weckhuysen, W. J. J. Huijgen, R. J. A. Gosselink, P. C. A. Bruijnincx, *Green Chem.* **2016**, *18*, 2651–2665.
[92] N. Li, Y. Li, C. G. Yoo, X. Yang, X. Lin, J. Ralph, X. Pan, *Green Chem.* **2018**, *20*, 4224–4235.
[93] W. Schutyser, T. Renders, S. Van Den Bosch, S. F. Koelewijn, G. T. Beckham, B. F. Sels, *Chem. Soc. Rev.* **2018**, *47*, 852–908.
[94] C. S. Lancefield, I. Panovic, P. J. Deuss, K. Barta, N. J. Westwood, *Green Chem.* **2017**, *19*, 202–214.
[95] T. Higuchi, T. Ito, T. Umezawa, T. Hibino, D. Shibata, *J. Biotechnol.* **1994**, *37*, 151–158.
[96] E. Fischer, A. Speier, *Chem. Ber.* **1895**, *28*, 3252–3258.
[97] L. Chen, J. Y. Zhu, C. Baez, P. Kitin, T. Elder, *Green Chem.* **2016**, *18*, 3835–3843.
[98] R. Wang, L. Chen, J. Y. Zhu, R. Yang, *ChemNanoMat* **2017**, *3*, 328–335.
[99] H. Zhou, J. Y. Xu, Y. J. Fu, H. G. Zhang, Z. W. Yuan, M. H. Qin, Z. J. Wang, *Green Chem.* **2019**, *21*, 4625–4632.
[100] D. M. Miles-Barrett, A. R. Neal, C. Hand, J. R. Montgomery, I. Panovic, O. S. Ojo, C. S. Lancefield, D. B. Cordes, A. M. Slawin, T. Lebl, *Org. Biomol. Chem.* **2016**, *14*, 10023–10030.
[101] S. A. Ralph, J. Ralph, L. Landucci, L. Landucci, *US Forest Prod. Lab., Madison, WI* (http://ars.usda.gov/Services/docs.htm), **2004**.
[102] T. L. Lohr, Z. Li, T. J. Marks, *ACS Catal.* **2015**, *5*, 7004–7007.
[103] F. Xu, J. X. Sun, R. Sun, P. Fowler, M. S. Baird, *Ind. Crops Prod.* **2006**, *23*, 180–193.
[104] P. Figueiredo, C. Ferro, M. Kemell, Z. Liu, A. Kiriazis, K. Lintinen, H. F. Florindo, J. Yli-Kauhaluoma, J. Hirvonen, M. A. Kostiainen, *Nanomedicine* **2017**, *12*, 2581–2596.
[105] J. Sun, C. Wang, L. P. Stubbs, C. He, *Macromol. Mater. Eng.* **2017**, *302*, 1700341.
[106] G. Appendino, A. Minassi, N. Daddario, F. Bianchi, G. C. Tron, *Org. Lett.* **2002**, *4*, 3839–3841.
[107] R. D. Offenhauser, *J. Chem. Educ.* **1964**, *41*, 39–40.
[108] H. Zhou, L. Tan, Y. Fu, H. Zhang, N. Liu, M. Qin, Z. Wang, *ChemSusChem* **2019**, *12*, 1213–1221.
[109] D. J. McClelland, P. H. Galebach, A. H. Motagamwala, A. M. Wittrig, S. D. Karlen, J. S. Buchanan, J. A. Dumesic, G. W. Huber, *Green Chem.* **2019**, *21*, 2988–3005.
[110] H. Lou, J. Y. Zhu, T. Q. Lan, H. Lai, X. Qiu, *ChemSusChem* **2013**, *6*, 919–927.
[111] T. Q. Lan, H. Lou, J. Y. Zhu, *BioEnergy Res.* **2013**, *6*, 476–485.
[112] J. Zhang, F. Gu, J. Y. Zhu, R. S. Zalesny, *Bioresour. Technol.* **2015**, *186*, 223–231.
[113] A. Smit, W. Huijgen, *Green Chem.* **2017**, *19*, 5505–5514.
[114] M. Yamamoto, M. Iakovlev, S. Bankar, M. S. Tunc, A. van Heiningen, *Bioresour. Technol.* **2014**, *167*, 530–538.
[115] H. Chen, X. Zhao, D. Liu, *ACS Sustainable Chem. Eng.* **2016**, *4*, 6668–6679.
[116] W. Wang, F. Gu, J. Y. Zhu, K. Sun, Z. Cai, S. Yao, W. Wu, Y. Jin, *Ind. Crops Prod.* **2020**, *150*, 112423.
[117] A. Kallioinen, M. Hakola, T. Riekkola, T. Repo, M. Leskelä, N. Von Weymarn, M. Siika-aho, *Bioresour. Technol.* **2013**, *140*, 414–420.
[118] U. F. Rodríguez-Zúñiga, D. Cannella, R. D. C. Giordano, R. D. L. C. Giordano, H. Jørgensen, C. Felby, *Green Chem.* **2015**, *17*, 2896–2903.
[119] A. M. Da Costa Lopes, R. M. G. Lins, R. A. Rebelo, R. M. Łukasik, *Green Chem.* **2018**, *20*, 4043–4057.
[120] Y. Liu, J. Zheng, J. Xiao, X. He, K. Zhang, S. Yuan, Z. Peng, Z. Chen, X. Lin, *ACS Omega* **2019**, *4*, 19829–19839.
[121] E. Rojo, M. S. Peresin, W. W. Sampson, I. C. Hoeger, J. Vartiainen, J. Laine, O. J. Rojas, *Green Chem.* **2015**, *17*, 1853–1866.
[122] H. Bian, L. Chen, H. Dai, J. Y. Zhu, *Carbohydr. Polym.* **2017**, *167*, 167–176.
[123] C. Su, K. Hirth, Z. Liu, Y. Cao, J. Y. Zhu, *Ind. Crops Prod.* **2021**, *159*, 113017.
[124] C. Su, K. Hirth, Z. Liu, Y. Cao, J. Y. Zhu, *GCB Bioenergy* **2021**, *13*, DOI:10.1111/gcbb.12866.
[125] G. Gellerstedt, W. W. Al-Dajani, *Holzforschung* **2000**, *54*, 609–617.
[126] P. M. Froass, A. J. Ragauskas, J. E. Jiang, *J. Wood Chem. Technol.* **1996**, *16*, 347–365.
[127] W. Zhu, C. J. Houtman, J. Y. Zhu, R. Gleisner, K. F. Chen, *Process Biochem.* **2012**, *47*, 785–791.
[128] H. Bian, J. Luo, R. Wang, X. Zhou, S. Ni, R. Shi, G. Fang, H. Dai, *ACS Sustainable Chem. Eng.* **2019**, *7*, 20022–20031.
[129] Y. M. Questell-Santiago, M. V. Galkin, K. Barta, J. S. Luterbacher, *Nat. Chem. Rev.* **2020**, *4*, 311–330.
[130] T. Jeoh, M. J. Cardona, N. Karuna, A. R. Mudinoor, J. Nill, *Biotechnol. Bioeng.* **2017**, *114*, 1369–1385.
[131] L. R. S. Moreira, E. X. F. Filho, *Appl. Microbiol. Biotechnol.* **2016**, *100*, 5205–5214.
[132] Y. P. Wijaya, R. D. D. Putra, V. T. Widyaya, J.-M. Ha, D. J. Suh, C. S. Kim, *Bioresour. Technol.* **2014**, *164*, 221–231.
[133] R. Weingarten, J. Cho, W. C. Conner Jr, G. W. Huber, *Green Chem.* **2010**, *12*, 1423–1429.

Manuscript received: April 30, 2021
Revised manuscript received: May 24, 2021
Accepted manuscript online: May 25, 2021
Version of record online: July 14, 2021

© 2021 The Authors ChemSusChem
© 2021 Chemistry Europe and Wiley-VCH GmbH.
This article has been contributed to by US Government employees and their work is in the public domain in the USA.